DOI: 10.1002/ejic.200700072

The Aromatization of C_5 Rings on a Heteronuclear Cluster

Yong Leng Kelvin Tan[a] and Weng Kee Leong*[a]

Keywords: Heterometallic complexes / Ruthenium / Osmium / Carbocyclic rings / Cyclopentadienyl ligands

The reaction of the heteronuclear cluster $RuOs_3(\mu\text{-}H)_2(CO)_{13}$ with saturated and unsaturated C_5 rings led to the aromatization of the rings to afford the clusters $RuOs_3(\mu\text{-}H)(CO)_9(\mu\text{-}CO)_2(\eta^5\text{-}C_5R_4R')$. However, the reaction with cyclopentene gave the cluster $RuOs_3(\mu\text{-}H)_3(CO)_{11}(\mu,\eta^1\text{:}\eta^2\text{-}C_5H_7)$ via C–H activation of an sp^2 carbon instead. Thermolysis of two of the products, $RuOs_3(\mu\text{-}H)(CO)_9(\mu\text{-}CO)_2(\eta^5\text{-}Cp')$ and $RuOs_3(\mu\text{-}H)(CO)_9(\mu\text{-}CO)_2(\eta^5\text{-}C_5H_4SiMe_3)$, led to their isomerization to butterfly clusters.

(© Wiley-VCH Verlag GmbH & Co. KGaA, 69451 Weinheim, Germany, 2007)

Introduction

Carbocyclic ligands such as cyclopentadienyls are ubiquitous in organometallic chemistry, and many of their compounds are important as catalysts. Furthermore, these ligands have an important role in many catalytic processes, and establishing the nature of the ligand–metal interaction is important to an understanding of the catalytic reaction.[1] Transition-metal clusters incorporating unsaturated organic molecules can serve as useful models for comprehending these processes due to the similarities between ligand–cluster and absorbate–surface interactions. This has resulted in a well-developed chemistry of this class of compounds, and several reviews have been published.[2] In contrast to the extensive reports on the reactivity of homonuclear clusters with carbocyclic ligands, few examples exist for heteronuclear clusters. The synergistic effect of having different adjacent metals in heteronuclear clusters may offer higher activity, greater selectivity, and better stability than their homonuclear counterparts. We had earlier developed a high-yield synthetic route to the hetero group 8 tetranuclear cluster $RuOs_3(\mu\text{-}H)_2(CO)_{13}$ (**1**) and have initiated a series of investigations into the chemistry of **1** and its derivatives.[3,4] It is with an exploration of the reactivity of a heteronuclear cluster with C_5 carbocyclic rings in mind that we would like to report here the results of our investigations into the reaction of **1** with a number of representative saturated and unsaturated C_5 rings, particularly in relation to their binding and transformation on the cluster.

Results and Discussion

With the notable exception of cyclopentene, we have found that the reaction of **1** with a variety of cyclopentanes, cyclopentenes, and cyclopentadienes at 120 °C afforded tetrahedral clusters of the general formula $RuOs_3(\mu\text{-}H)(CO)_9(\mu\text{-}CO)_2(\eta^5\text{-}C_5R_4R')$ (**2**) in moderate to high yields; this is depicted in Scheme 1. Although aromatization of cyclohexene and cyclohexadiene on tetraosmium clusters are known,[5] this appears to be the first time that aromatization of C_5 rings, including even saturated ones, on clusters have been observed. All the clusters **2** have been characterized completely and, with the exception of **2c**, also by single-crystal X-ray crystallography. The synthesis of **2a** by the ionic coupling of $[Ru(C_5H_5)(MeCN)_3]^+$ with $[Os_3H(CO)_{11}]^-$ and its X-ray crystal structure have also been previously reported;[6] we are reporting our results here to minimize instrumental variations for purposes of comparison.

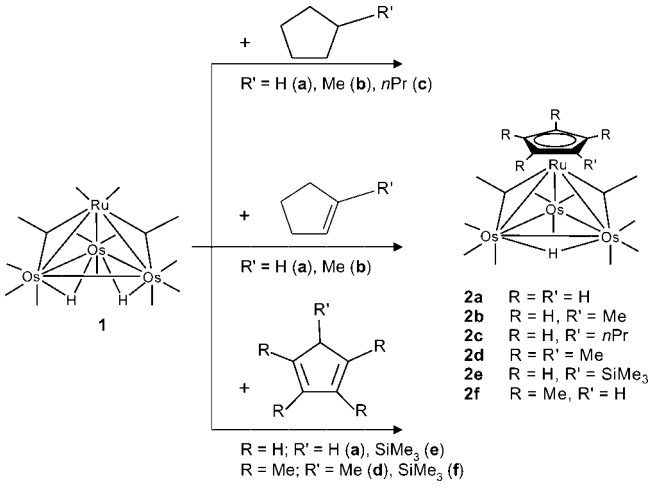

Scheme 1.

The ORTEP diagrams for **2d** and **2e** are shown in Figure 1, and a common atomic numbering scheme and selected bond parameters for the clusters **2** are given in Table 1. The clusters consist of a tetrahedral arrangement

[a] Department of Chemistry, National University of Singapore, Kent Ridge, 119260 Singapore

 © 2007 Wiley-VCH Verlag GmbH & Co. KGaA, Weinheim

of metal atoms; the three osmium atoms form the triangular basal plane and are capped by a ruthenium atom at the apex. The tetrahedral metal core with six metal–metal bonds is consistent with the valence electron count of 60 for the molecules. The longest metal–metal edge found in all of the clusters is bridged by a hydride ligand;[7] the Os(1)–Os(2) bond length ranges from 2.9413(6) to 3.0056(10) Å; the other metal–metal bond lengths in the clusters range from 2.7709(7) to 2.9060(12) Å. There are two asymmetric bridging carbonyl groups which span the Os(1)–Ru(4) and Os(2)–Ru(4) edges; the bond to the ruthenium atom [average 1.97(2) Å] is shorter than that to the osmium atom [average 2.26(4) Å]. Bridging carbonyl groups are better π-acceptors than terminal CO groups, and their presence helps to disperse the additional electron density contributed by the electron-rich Ru(η^5-cyclopentadienyl) fragment.[8]

The organic moiety in **2** is coordinated to the cluster at the apical ruthenium atom via the conventional η^5-cyclopentadienyl bonding mode. It is noted that cyclopentadienyl ligand substitution occurs overwhelmingly at the ruthenium vertex, in line with previous reports of group 15 derivatives of cluster **1**.[3] There is no evidence for the presence of an isomer with the carbocyclic ligand ligating an osmium ver-

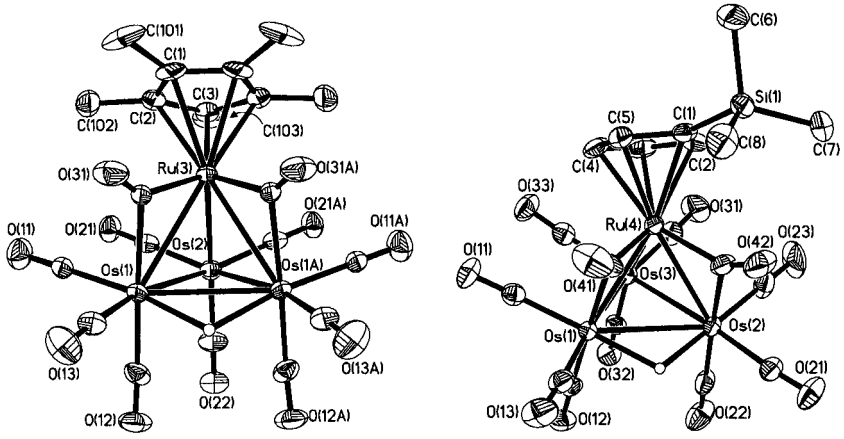

Figure 1. ORTEP diagram (50% probability thermal ellipsoids, organic hydrogen atoms omitted) for **2d** (left) and **2e** (right).

Table 1. Common atomic numbering scheme and selected bond parameters for **2**.

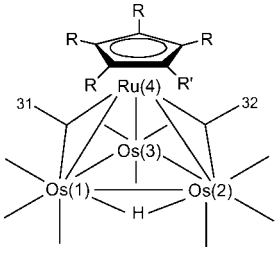

2a R = R' = H
2b R = H, R' = Me
2c R = H, R' = $CH_2CH_2CH_3$
2d R = R' = Me
2e R = H, R' = $SiMe_3$
2f R = Me, R' = H

	2a Molecule A	Molecule B	**2b**	**2d**	**2e**	**2f**
Bond lengths [Å]						
Os(1)–Os(2)	2.9458(6)	2.9470(6)	2.9428(4)	2.9413(6)	2.9425(3)	3.0056(10)
Os(1)–Os(3)	2.7853(7)	2.7789(7)	2.7872(3)	2.7781(4)	2.7848(3)	2.8434(7)
Os(1)–Ru(4)	2.7933(10)	2.8292(11)	2.8168(5)	2.8571(7)	2.8278(4)	2.9060(12)
Os(2)–Os(3)	2.7709(7)	2.7907(7)	2.7872(3)	2.7781(4)	2.7732(3)	2.8434(7)
Os(2)–Ru(4)	2.8319(10)	2.8042(10)	2.8168(5)	2.8571(7)	2.8322(4)	2.9060(12)
Os(3)–Ru(4)	2.7705(10)	2.7693(10)	2.7721(6)	2.8055(9)	2.7906(4)	2.8609(13)
Os(1)–C(31)	2.187(11)	2.253(13)	2.315(5)	2.244(8)	2.253(5)	2.297(11)
Ru(4)–C(31)	2.007(12)	1.971(13)	1.965(5)	1.960(7)	1.967(6)	1.997(11)
Os(2)–C(32)	2.254(12)	2.228(13)	2.231(5)	2.244(8)	2.272(5)	2.297(11)
Ru(4)–C(32)	1.947(14)	1.967(13)	1.965(5)	1.960(7)	1.946(5)	1.997(11)
Ru(4)–Cp(centroid)	1.918(18)	1.923(18)	1.905(17)	1.925(8)	1.896(5)	1.948(11)
Bond angles [°]						
Os(1)–C(31)–Ru(4)	83.4(5)	83.8(5)	84.1(2)	84.4(3)	83.8(2)	84.9(4)
Os(2)–C(32)–Ru(4)	84.4(5)	83.6(4)	84.1(2)	84.4(3)	84.0(2)	84.9(4)

 © 2007 Wiley-VCH Verlag GmbH & Co. KGaA, Weinheim

tex. This preference for substitution at a ruthenium vertex is electronic; it cannot be statistical since that would lead to a 3:1 preference for substitution at an osmium vertex.

As has been observed for $Os_4(\mu\text{-H})(CO)_9(\mu\text{-CO})_2(\eta^5\text{-Cp*})$, one of the methyl carbon atoms in **2d** [C(103) in the ORTEP diagram] is displaced out of the plane of the central carbon ring of the pentacyclopentadienyl ligand by 18°. The displacement of the other methyl carbon atoms from the carbon ring plane for this cluster averages 7°. This bending of the methyl carbon atom has been ascribed to the steric interaction of the methyl group with the nearest carbonyl groups.[9] The presence of bridging carbonyl ligands results in a reduction of the distance as well as an increase in the nonbonding interaction between the oxygen atom of the CO ligand and any bulky substituents on the cyclopentadienyl ring, giving rise to bridging carbonyl-substituted cyclopentadienyl ring repulsion. This can be seen in **2e**, where the bulky trimethylsilyl group is placed directly above and between the two bridging carbonyl ligands to minimize steric strain, while the cyclopentadienyl ring is tilted at an angle of 36° with respect to the triosmium basal plane.

Steric reasons may also account for the fact that the cluster $RuOs_3(\mu\text{-H})(CO)_9(\mu\text{-CO})_2(\eta^5\text{-}C_5Me_4SiMe_3)$ was not isolated in the reaction of **1** with trimethyl(2,3,4,5-tetramethyl-2,4-cyclopentadien-1-yl)silane. Instead the major products isolated from the reaction were **2f**, in which the trimethylsilyl group was lost, and another species $RuOs_3(\mu\text{-H})_3(CO)_8(\mu\text{-CO})(\eta^5\text{-}C_5Me_4SiMe_3)$ (**4**) (see below). The steric crowding around the C_5Me_4H ring in **2f** is reflected by the out-of-plane displacement of the methyl groups (average 6°) away from the $RuOs_3$ core. The cyclopentadienyl ring is also tilted at an angle of 36° with respect to the triosmium basal plane. The presence of an additional bulky trimethylsilyl substituent would have resulted in an even larger displacement of the silicon and methyl carbon atoms out of the plane of the cyclopentadienyl ring. This steric strain may similarly account for our observation that prolonged thermolysis of pentaphenylcyclopentadiene with **1** failed to give the expected product $RuOs_3(\mu\text{-H})(CO)_9(\mu\text{-CO})_2(\eta^5\text{-}C_5Ph_5)$, but resulted in the recovery of **1**.

The clusters appear to retain their solid-state structures in solution. The singlet resonance in the high-field region for the hydride shows a systematic downfield shift with increasing number of electron donating groups (such as methyl) on the cyclopentadienyl ring. Furthermore, a comparison of the hydride chemical shift for **2d** (δ = –18.34 ppm) with that reported for the tetraosmium analogue, $Os_4(\mu\text{-H})(CO)_9(\mu\text{-CO})_2(\eta^5\text{-Cp*})$ (δ = –20.71 ppm),[9] shows that replacement of the osmium atom at the apex of the tetrahedron with the relatively more electronegative ruthenium atom results in a decrease in electron density at the hydride.[10]

Some of the reactions with the C_5 carbocyclic rings also afforded other minor products other than **2**. The reaction of **1** with propylcyclopentane afforded, after TLC separation, unreacted **1**, $Os_3(\mu\text{-H})_2(CO)_{10}$ (a decomposition product of **1**), **2c**, and another novel cluster $Ru_2Os_3(\mu\text{-H})_2(CO)_{13}(\mu\text{-CO})(\mu_3,\eta^5\text{:}\sigma^2\text{-}C_5H_3C_3H_7)$ (**3**). Clusters **2c** and **3** could not be separated by chromatographic methods although NMR integration suggested that they were present in a ratio of 5:2. We managed to obtain some pure samples by fractional crystallization. Cluster **3** has been completely characterized, also by a single-crystal X-ray crystallographic study; the ORTEP diagram showing the molecular structure of **3** is depicted in Figure 2, together with selected bond parameters.

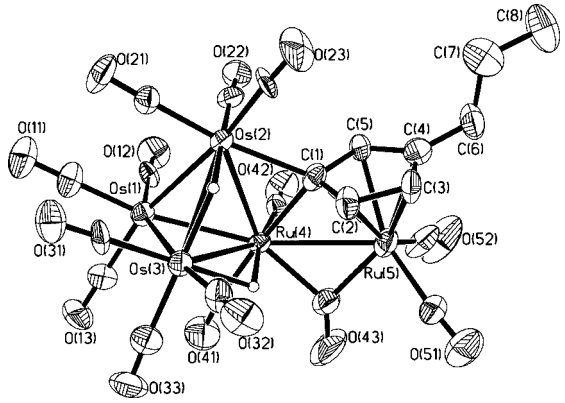

Figure 2. ORTEP diagram (50% probability thermal ellipsoids, organic hydrogen atoms omitted) and selected bond lengths [Å] and angles [°] for **3**. Os(1)–Os(2) = 2.8420(11); Os(1)–Os(3) = 2.7746(11); Os(1)–Ru(4) = 2.7729(17); Os(2)–Os(3) = 2.9572(11); Os(2)–Ru(4) = 2.8291(16); Os(3)–Ru(4) = 2.9571(17); Ru(4)–Ru(5) = 2.933(2); Os(2)–C(1) = 2.217(19); Ru(4)–C(1) = 2.30(2); Ru(5)–Cp(centroid) = 1.90(2); Ru(4)–C(43) = 2.08(2); Ru(5)–C(43) = 2.09(2); Os(2)–C(1)–Ru(4) = 77.5(7); Ru(4)–C(43)–Ru(5) = 89.5(9).

The metal framework in **3** consists of a ruthenium-spiked $RuOs_3$ tetrahedron. In metal carbonyl chemistry the spiked tetrahedron metal framework has been rarely reported. Amongst the few known clusters with this arrangement are $Os_6(\mu\text{-H})(\eta^2\text{-}C_6F_5NNNC_6F_5)(\mu\text{-CO})(CO)_{19}$,[11] $ReOs_4(\mu\text{-H})(\mu\text{-CO})(CO)_{17}$,[12] $RuOs_4(\mu\text{-H})_3(\mu_3\text{-}\eta^6\text{-}C_6H_5)(CO)_{12}[P(OMe)_3]$[13] and $Ru_2Os_3(\mu\text{-H})(\mu_3\text{-}\eta^5\text{-}C_5H_4)(\eta^5\text{-}C_5H_5)(CO)_{11}[P(OMe)_3]$.[14] The spike Ru(4)–Ru(5) edge at 2.933(2) Å in **3** is long despite its being bridged by a carbonyl group; usually the shortest metal–metal distance is associated with a bridging CO. For the metal tetrahedron, the two longest metal–metal bonds are bridged by metal hydrides [Os(2)–Os(3) and Os(3)–Ru(4), at 2.9572(11) and 2.9571(11) Å, respectively], whereas the other metal–metal vectors are significantly shorter [2.7729(11)–2.8420(11) Å]. The propylcyclopentadienylidene ligand is bonded to Os(2), Ru(4), and Ru(5) via an uncommon $\mu_3,\eta^5\text{:}\sigma^2$ mode; the ligand caps Ru(5) in a η^5-cyclopentadienyl manner, and C(1) is also asymmetrically bound to Os(2) [2.217(19) Å] and Ru(4) [2.30(2) Å]. The C(1) carbon acts as a one-electron donor, and the coordination of this atom to the Os(2)–Ru(4) edge can be considered as a "three-center-two-electron" bond. This gives **3** a cluster valence electron count of 76, consistent with the observed spiked tetrahedron metal core.[15] Cluster **3** can be envisaged as having been formed by the addition of a "$Ru(\eta^5\text{-}C_5H_4C_3H_7)(CO)_2$" fragment, from decomposition of **2c**, to **1** followed by oxidative addition of the substituted cyclopentadienyl group; the reaction of **1** with **2c** indeed afforded **3**.

 © 2007 Wiley-VCH Verlag GmbH & Co. KGaA, Weinheim

The ^{1}H NMR spectrum, in the hydride region, of **3** indicated the presence of three species, together with **2c**. The major species exhibited a broad singlet at –19.54 ppm (I); the two other sets comprised singlets at –20.73 and –21.70 ppm (II) and at –20.74 and –21.62 ppm (III). We were unable to obtain a pure sample of **3** free of **2c**, and the relative intensities of the other resonances remained unchanged across repeated recrystallizations. Integration of the spectrum taken at 198 K indicated the ratio I/II/III to be 4.6:2.7:1.0. Below 233 K, the signals due to I appeared as two sharp singlets at –19.06 and –20.12 ppm; the other signals showed no variation except for minor changes in chemical shifts due to temperature. The major resonances (I) can be attributed to the solid-state structure, and the EXSY spectrum at 198 K confirmed the chemical exchange between the two hydride resonances. The identities of the species giving rise to the other two sets of resonances are uncertain, but there was an absence of crosspeaks involving these resonances, and the chemical shift ranges indicated that these hydrides may be bridging Os–Os bonds.[16]

As already mentioned above, besides **2f**, the reaction with trimethyl(2,3,4,5-tetramethyl-2,4-cyclopentadien-1-yl)silane also afforded $RuOs_3(\mu\text{-}H)_3(CO)_9(\mu\text{-}CO)(\eta^5\text{-}C_5Me_4SiMe_3)$ (**4**), which has also been completely characterized, also by a single-crystal X-ray diffraction analysis; the ORTEP plot together with selected bond parameters is shown in Figure 3.

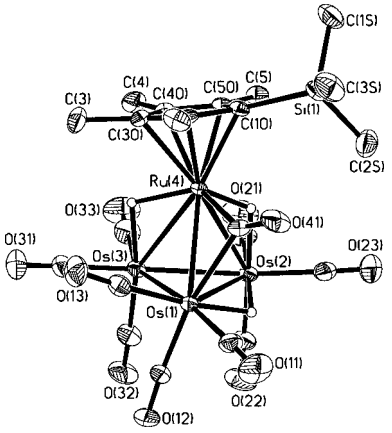

Figure 3. ORTEP diagram (50% probability thermal ellipsoids, organic hydrogen atoms omitted) and selected bond lengths [Å] and angles [°] for **4**. Os(1)–Os(2) = 2.9454(3); Os(1)–Os(3) = 2.8153(3); Os(1)–Ru(4) = 2.8292(4); Os(2)–Os(3) = 2.7988(3); Os(2)–Ru(4) = 2.9612(4); Os(3)–Ru(4) = 2.9626(4); Os(1)–C(41) = 2.208(5); Ru(4)–C(41) = 1.949(5); Ru(4)–Cp(centroid) = 1.840(5); Ru(4)–C(41)-Os(1) = 85.53(19).

The silicon atom of the $C_5Me_4SiMe_3$ ligand is displaced by 9°, while the four methyl groups are displaced at an average of 5°, out of the plane of the central carbon ring. These indicate that the replacement of a carbonyl ligand with two bridging hydrides enabled the cyclopentadienyl ring to coordinate to the metal tetrahedron with less steric strain, and may explain why the $SiMe_3$ group was retained, unlike in **2f**.

The ambient temperature ^{1}H NMR spectrum in the hydride region of **4** comprised a sharp singlet at –18.46 ppm. At 183 K, this was replaced by broad resonances centered at –16.95 ppm (A), –18.62 (B), and –20.75 (C), as well as a relatively sharper resonance at –21.07 ppm (D), in an integration ratio A/B/C/D of 8:2:1:4. These resonances may be ascribed to two inter-converting isomers existing in a 4:1 ratio; their proposed structures and tentative assignments are given in Figure 4. It is assumed that the major isomer has the structure as that in the X-ray crystallographic study, and that the resonances due to the two hydrides bridging the Ru–Os edges have collapsed into one broad resonance even at 183 K. The proposed structure of the minor isomer is based on the reported structures of $WM_3(\mu\text{-}H)_3(CO)_{11}(\eta^5\text{-}L)$ (M = Os or Ru, L = C_5H_5 or C_5Me_5).[17] The poor solubility of **4** at low temperatures precluded any attempt at studying the hydride exchange pathways further.

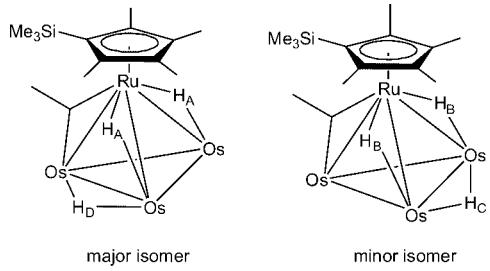

Figure 4. Proposed structures and tentative ^{1}H NMR assignments (hydride region) for **4**.

Among the reactions giving rise to clusters **2**, however, the most interesting was that involving the reaction with cyclopentene. The yield of **2a** from this reaction in refluxing octane was rather low (10%). In contrast, the reaction carried out at 120 °C in a Carius tube with hexane as solvent afforded an orange product in essentially quantitative yield, which was identified as the novel cluster $RuOs_3(\mu\text{-}H)_3(CO)_{11}(\mu,\eta^1\text{:}\eta^2\text{-}C_5H_7)$ (**5**). Attempts at purification by TLC on silica led to decomposition. Cluster **5** has been completely characterized, also by a single-crystal X-ray crystallographic analysis. An ORTEP plot of **5** showing the atomic numbering scheme, together with selected bond parameters, is given in Figure 5.

The crystal structure exhibits disorder of the metal framework, with ruthenium occupancies on the M(4) and M(1) positions refined to about 0.88 and 0.12, respectively. The cyclopentenyl ligand bridges one of the metal–metal edges in a $\mu,\eta^1\text{:}\eta^2$ manner. This bonding mode has been previously encountered, for example, in $Os_4(\mu\text{-}H)_3(CO)_{11}(\mu,\eta^1\text{:}\eta^2\text{-}C_6H_9)$,[2b,18] $Os_4(\mu\text{-}H)_3(CO)_{11}(\mu,\eta^1\text{:}\eta^2\text{-}CHCHPh)$,[19] $Os_3(\mu\text{-}H)(CO)_{10}(\mu,\eta^1\text{:}\eta^2\text{-}CHCHCH_2CH_3)$, $Os_3(\mu\text{-}H)(CO)_{10}(\mu,\eta^1\text{:}\eta^2\text{-}CHCH_2)$, and $Os_3(\mu\text{-}H)(CO)_{10}(\mu,\eta^1\text{:}\eta^2\text{-}CHCHPh)$.[20] The alkene C=C bond [1.392(9) Å], is elongated with respect to the typical alkene bond length of 1.33 Å,[21] consistent with a decrease in the bond order. The hydrides were placed by potential energy calculations[22] and are consistent with the elongation of the bridged metal–metal bonds.[23] Moreover, the M–M–C angles for CO ligands adjacent to, and in the same plane as, the bridging hydrides are observed to be abnormally large, ranging from 116 to 122°, relative to usual M–M–C angles of 70 to

 © 2007 Wiley-VCH Verlag GmbH & Co. KGaA, Weinheim

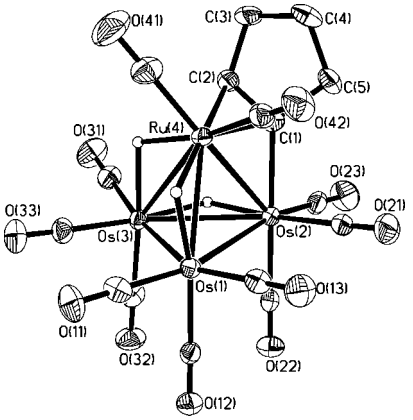

Figure 5. ORTEP diagram (50% probability thermal ellipsoids) and selected bond lengths [Å] and angles [°] for **5**. Os(1)–Os(2) = 2.9252(3); Os(1)–Os(3) = 2.7903(4); Os(1)–Ru(4) = 2.8020(5); Os(2)–Os(3) = 2.9763(4); Os(2)–Ru(4) = 2.7974(5); Os(3)–Ru(4) = 2.9452(5); Os(2)–C(1) = 2.112(7); Ru(4)–C(1) = 2.172(6); Ru(4)–C(2) = 2.307(7); C(1)–C(2) = 1.392(9); Os(2)–C(1)–Ru(4) = 81.5(2).

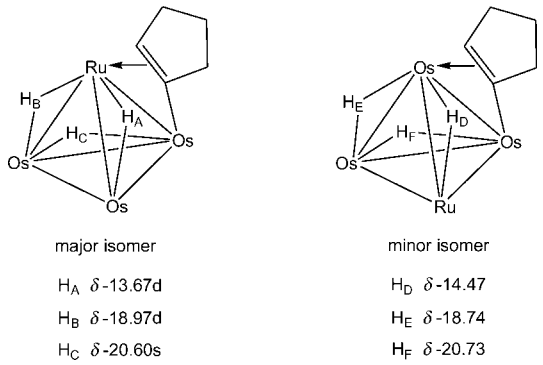

Figure 6. Proposed solution structures (carbonyl groups omitted) for the isomers of **5** and tentative NMR assignments for the bridging hydrides.

95°. This provides additional evidence for the location of the bridging hydride ligands. As has been observed in the case of $Os_4(\mu\text{-}H)_3(CO)_{11}(\mu,\eta^1\text{:}\eta^2\text{-}C_6H_9)$ and $Os_4(\mu\text{-}H)_3(CO)_{11}(\mu,\eta^1\text{:}\eta^2\text{-}CHCHPh)$,[18b] one of the longer metal–metal bonds is not bridged [Os(1)–Os(2) = 2.9252(3) Å].

The ^1H resonances for the organic moiety have been tentatively assigned with the aid of COSY and NOESY experiments, and the coupling constants have been determined by selective decoupling experiments. The ^1H NMR spectrum in the high-field region suggested the presence of two isomers in a 9:1 ratio, consistent with the disorder ratio observed in the solid-state crystal structure. The major set of resonances consists of doublets at –13.67 and –18.97 ppm, and a singlet at –20.60 ppm. The H–H coupling has been confirmed by COSY and selective decoupling experiments. The resonances of the minor isomer were very low in intensity and appeared as singlets. We have tentatively assigned the resonances as shown in Figure 6. The assignments were corroborated by a NOESY spectrum which showed a crosspeak between the resonances at –18.97 and –20.60 ppm, indicating spatial proximity of the hydrides giving rise to them.

In addition to the two sets of resonances described above, the ^1H NMR spectrum of **5** at ambient temperature displayed two broad signals at –19.70 and –21.20 ppm, suggesting the presence of another fluxional species. A variable-temperature experiment showed that at 213 K, three singlet resonances at –19.33, –20.41, and –21.41 ppm resulted. An EXSY experiment (213 K and 343 K) indicated exchange crosspeaks between the first two resonances, but no intermolecular exchange was observed between this species and either isomer of **5**. Together with the rather different chemical shifts for these hydrides relative to the others, this species may be unrelated to **5**, although at this point in time a structure cannot be unambiguously assigned.

The EXSY experiment at 343 K also indicated hydride fluxionality in each of the two isomers of **5** but no isomerization between them. Two fluxional processes that can account for the exchange crosspeaks in the major isomer are depicted in Scheme 2. Both processes involve rapid reorientation of the cyclopentenyl moiety about the Ru–Os edge; a similar process has earlier been proposed for the norbornene triosmium cluster $Os_3(\mu\text{-}H)(CO)_{10}(\mu,\eta^1\text{:}\eta^2\text{-}C_7H_9)$.[24] In process I, the flipping of H_C from one Os–Os edge to another, coupled with the reorientation of the cyclopentenyl ligand interchanges H_A and H_B. The movement of the organic moiety together with simultaneous flipping of all three hydrides in process II exchanges H_A with H_C. Process I is expected to occur at a faster rate than II, and this is supported by the variable-temperature NMR spectra, which show that the signals ascribable to H_A and H_B broaden more rapidly than that attributable to H_C. This is further supported by the more intense exchange crosspeak between H_A and H_B; the weaker intensity of the exchange crosspeak between H_B and H_C may be attributed to a combination of processes I and II.

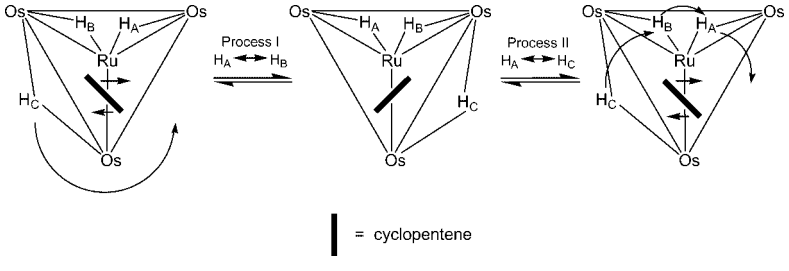

Scheme 2.

 © 2007 Wiley-VCH Verlag GmbH & Co. KGaA, Weinheim

The interesting question is why the reaction of **1** with cyclopentene should afford only **5**. This is particularly in contrast with the reaction with methylcyclopentene, which afforded **2b** in comparatively good yield. Furthermore, no methylcyclopentenyl analogue of **5** could be identified spectroscopically despite attempts to decrease the reaction time or temperature. It is tempting to view cluster **5** as a possible precursor to **2a**; indeed, heating a sample of **5** in hexane for 12 h afforded **2a**. However, the low yield (20%) and the great number of side products obtained from this thermolysis seem to indicate that this is not so. The transformation of **5** to **2a** would require not only dehydrogenation but also the rehydrogenation of the metallated carbon atom. This situation is similar to that in the related tetraosmium cluster $Os_4(\mu\text{-}H)_3(CO)_{11}(\mu,\eta^1\text{:}\eta^2\text{-}C_6H_9)$,[18c] which was determined not to be an active intermediate in the dehydrogenation of the cluster-bound cyclohexa-1,3-diene to give $Os_4(\mu\text{-}H)_2(CO)_{10}(\eta^6\text{-}C_6H_6)$.[2c] We believe that **5** was formed preferentially because of faster C–H activation of an sp^2 carbon than an allylic sp^3 carbon;[25] the latter is what would be required for aromatization to **2a**.

The reason why methylcyclopentene failed to give an analogue to **5** is probably steric; the hydrogen atom on C(2) (which is where the methyl substituent would be) points towards CO(31) in **5** (Figure 5). In the case of the dienes, presumably the fact that one C–H activation at an sp^3 carbon would be sufficient to bring about aromatization may have tilted the balance against the formation of an analogue of **5**. This is corroborated by the observation that to date, only $Os_3(CO)_{10}(\eta^4\text{-}C_5H_6)$, obtained in the reaction of $Os_3(CO)_{10}(MeCN)_2$ with cyclopentadiene in dichloromethane, has been successfully characterized by infrared spectroscopy; in the absence of excess cyclopentadiene the cluster decomposed rapidly.[26]

The clusters **2** have also been subjected to thermolysis in cyclohexane. While **2a**, **2d**, and **2f** were found to be thermally stable, **2b** and **2e** afforded the novel products $RuOs_3(\mu\text{-}H)_2(CO)_{11}(\mu,\eta^5\text{:}\eta^1\text{-}C_5H_3Me)$(**6b**)and$RuOs_3(\mu\text{-}H)_2(CO)_{11}(\mu,\eta^5\text{:}\eta^1\text{-}C_5H_3SiMe_3)$ (**6e**) respectively. Both **6b** and **6e** have been completely characterized by spectroscopic, elemental, and single-crystal X-ray crystallographic analyses. An ORTEP plot of the molecular structure of **6e** is displayed in Figure 7; selected bond parameters for **6b** and **6e** are given in Table 2, together with a common atomic numbering scheme. There were two molecules in the asymmetric unit of **6b**.

Clusters **6b** and **6e** are isomers of **2b** and **2e**, respectively, in which it may be considered that oxidative addition of a C–H bond of the cyclopentadienyl across a metal–metal bond has occurred, so that the resulting ligand bridges the wingtip metal atoms of a butterfly cluster core. The cluster valence electron count of 62 for these clusters is consistent with the butterfly structure. The dihedral angle between the two "wings" of the butterfly – the Ru(4)–Os(1)–Os(3) and Os(1)–Os(2)–Os(3) planes – is 87.8° for **6b** and 88.6° for **6e**. While the Os(1)–Os(3) bonds in **6b** [3.0488(5) Å, molecule A; 3.0451(5) Å, molecule B] as well as **6e** [3.0212(3) Å] show the lengthening associated with a metal–metal vector bridged by a hydride ligand,[7] the hinge bond [2.7948(5)–2.8004(3) Å] is short despite the presence of a bridging hydride. Similar behavior has been observed for the tetraosmium butterfly clusters $Os_4(\mu\text{-}H)_2(CO)_{13}(PMe_3)$ and $Os_4(\mu\text{-}H)(CO)_{12}(Cp^*)$,[27,28] and this has been attributed to the different coordination numbers of the metal atoms; without exception, the osmium atoms linked to only three terminal ligands in these tetraosmium clusters are associated with shorter metal–metal bond lengths.

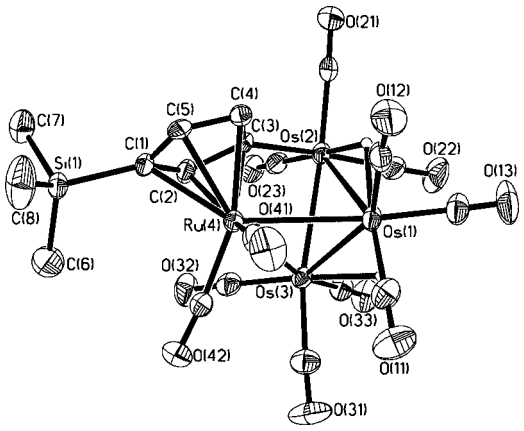

Figure 7. ORTEP diagram (50% probability thermal ellipsoids, organic hydrogen atoms omitted) for **6e**.

Table 2. Common atomic numbering scheme and selected bond parameters for **6b** and **6e**.

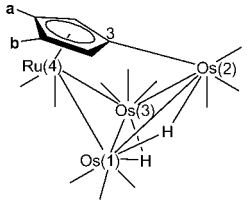

	a	**b**
6b	H	Me
6e	$SiMe_3$	H

Bond lengths [Å]	**6b** (Molecule A)	**6b** (Molecule B)	**6e**
Os(1)–Os(2)	3.0488(5)	3.0451(5)	3.0212(3)
Os(1)–Os(3)	2.7953(5)	2.7948(5)	2.8009(3)
Os(1)–Ru(4)	2.9043(10)	2.9111(10)	2.9172(5)
Os(2)–Os(3)	2.8289(5)	2.8335(5)	2.8527(3)
Os(3)–Ru(4)	2.9469(9)	2.9367(9)	2.9393(4)
Os(2)–C(3)	2.122(11)	2.120(12)	2.096(5)
Ru(4)–Cp(centroid)	1.880(11)	1.880(11)	1.886(5)
Bond angles [°]			
Os(2)–C(3)–Cp(centroid)	168.55	167.16	169.67

The ^1H NMR spectrum for **6e** indicated that the solid-state structure persisted in solution. In contrast, the ambient-temperature ^1H NMR spectrum of **6b** showed a broad singlet at –17.05 ppm. On prolonged standing in solution, the compound isomerized to **2b**, as well as decomposing into some unidentified products. On cooling **6b** to 183 K, we observed three sets of resonances, which may be attributed to the presence of three isomers. However, it is not possible to assign solution-state structures for these isomers unambiguously.

 © 2007 Wiley-VCH Verlag GmbH & Co. KGaA, Weinheim

Concluding Remarks

Our investigations show that thermolysis of **1** with both saturated and unsaturated C_5 rings led to ring aromatization via C–H activation and/or loss of a trimethylsilyl moiety, resulting in the formation of clusters **2**; binding of the resulting cyclopentadienyl moiety was specifically at the ruthenium vertex. Loss of the trimethylsilyl group appeared to be dictated by steric factors, so that two products were formed in the reaction with trimethyl(2,3,4,5-tetramethyl-2,4-cyclopentadien-1-yl)silane, viz., **2f** via loss of the silyl group, or **4** via loss of a carbonyl. The reaction with cyclopentene gave, in high yields, the unusual cluster **5** via C–H activation at an sp^2 carbon rather than aromatization of the cyclopentene via activation of an allylic sp^3 carbon, and again steric reason seemed to explain the fact that an analogue was not observed in the case of 1-methylcyclopentene. Under prolonged thermolysis, cluster fragmentation and condensation can occur, and this accounts for the low yields of **2** observed in some of the reactions.

Experimental Section

General Procedures: All reactions and manipulations were carried out under nitrogen by using standard Schlenk techniques. Solvents were purified, dried, distilled, and stored under nitrogen prior to use. The products were separated by thin layer chromatography (TLC), using plates coated with silica gel 60 F254 of 0.25 or 0.5 mm thickness and extracted with dichloromethane. Routine NMR spectra were acquired with a Bruker ACF300 NMR spectrometer, while decoupling, variable-temperature and 2D NMR spectra were obtained with a Bruker Avance DRX500 or Bruker AMX500 machine. EXSY spectra were recorded with a mixing time of 0.5 s unless otherwise stated. The solvent used was deuterated chloroform unless otherwise stated. ^{1}H chemical shifts reported are referenced against the residual proton of the solvents. Mass spectra were obtained with a Finnigan MAT95XL-T spectrometer in an *m*-nitrobenzyl alcohol matrix. Microanalyses were carried out by the microanalytical laboratory at the National University of Singapore. The preparation of cluster **1** appears in our earlier report.[3a] All other reagents were from commercial sources and used as supplied.

Reactions of $RuOs_3(\mu\text{-}H)_2(CO)_{13}$ (1) with C_5 Rings: In a typical reaction, to a solution of **1** in the solvent in a Carius tube was added an excess of the substrate. The solution was degassed by three freeze-pump-thaw cycles and heated. The solvent was removed under reduced pressure, and the residue so obtained was redissolved in the minimum of dichloromethane and chromatographed on TLC plates with hexane/dichloromethane (3:2, v/v) as the mobile phase. The reaction conditions and yields are summarized in Table 3, and the spectroscopic and analytical data for the products are in Table 4 and Table 5.

Reaction of 1 with Cyclopentene: To a Carius tube containing **1** (20.5 mg, 0.020 mmol) and hexane (30 mL) was added cyclopentene (0.1 mL). The reaction mixture was degassed by three freeze-pump-thaw cycles and stirred at 120 °C for 12 h, after which the solvent was removed under reduced pressure. Recrystallization of the red solid in hexane/dichloromethane gave dark orange crystals of **5** as the sole product (19.7 mg, 95%).

Thermolysis of $RuOs_3(\mu\text{-}H)_3(CO)_{11}(\mu,\eta^1\text{:}\eta^2\text{-}C_5H_7)$ (5): To a Carius tube containing hexane (30 mL) was added **5** (10.1 mg, 0.010 mmol). The reaction mixture was degassed by three freeze-pump-thaw cycles and stirred at 120 °C for 12 h, after which the solvent was removed under reduced pressure. The residue so obtained was redissolved in the minimum of dichloromethane and chromatographed on TLC plates. Elution with hexane/dichloromethane (7:3, v/v) gave a plethora of products, amongst which **2a** was identified (2.1 mg, 20%).

Reaction of 1 with 2c: To a Carius tube containing hexane (30 mL) was added **1** (8.2 mg, 0.079 mmol) and **2c** (5.1 mg, 0.047 mmol). The reaction mixture was degassed by three freeze-pump-thaw cycles and stirred at 120 °C for 24 h, after which the solvent was removed under reduced pressure. The residue so obtained was redissolved in the minimum of dichloromethane and chromatographed on TLC plates. Elution with hexane/dichloromethane (7:3,

Table 3. Reaction conditions and yields for the reaction of **1** with C_5 rings.

Amount of **1**	Substrate (volume)	Conditions	Prod.	R_f	Color	Yield
16.7 mg 0.016 mmol	cyclopentane (20 mL)	120 °C, 24 h	**2a**	0.56	dark brown	7.5 mg (45%)
18.2 mg, 0.018 mmol	cyclopentene (0.1 mL)	octane (20 mL), reflux, 12 h	**2a**	0.56	dark brown	1.9 mg (10%)
20.7 mg, 0.020 mmol	cyclopentadiene (0.1 mL)	hexane (30 mL), 120 °C, 12 h	**2a**	0.56	dark brown	13.7 mg (66%)
7.5 mg, 0.008 mmol	1-methyl-1-cyclopentane (5.0 mL)	120 °C, 24 h	**2b**	0.44	dark brown	6.3 mg (74%)
20.6 mg, 0.020 mmol	1-methyl-1-cyclopentene (0.1 mL)	hexane (30 mL), 120 °C, 12 h	**6b**	0.48	dark brown	4.4 mg (14%)
			2b	0.44	dark brown	8.2 mg (39%)
20.2 mg, 0019 mmol	propylcyclopentane (0.1 mL)	cyclohexane (30 mL), 120 °C, 40 h	**3**	0.46	orange	8.3 mg (40%)
			2c	0.46	orange	(**2c**/**3** = 5:2)
23.6 mg, 0.023 mmol	pentamethylcyclopentadiene (0.1 mL)	hexane (30 mL), 120 °C, 12 h	**2d**	0.63	dark brown	17.0 mg (67%)
21.2 mg, 0.020 mmol	(trimethyl silyl)cyclopentadiene (0.5 mL)	cyclohexane (30 mL), 120 °C, 20 h	**6e**	0.56	orange	8.5 mg (42%)
			2e	0.36	orange	9.0 mg (45%)
30.1 mg, 0.029 mmol	trimethyl[2,3,4,5-tetramethyl-2,4-cyclopentadien-1-yl]-silane (0.5 mL)	hexane (30 mL), 120 °C, 20 h	**4**	0.56	dark red	7.8 mg (23%)
			2f	0.47	dark red	8.1 mg (25%)

 © 2007 Wiley-VCH Verlag GmbH & Co. KGaA, Weinheim

Table 4. Infrared spectroscopy and elemental analysis data for **2**–**6**.

Cluster	IR (CH_2Cl_2) ν(CO) [cm^{-1}]	Elemental analysis [%] found (calculated)
2a	2089m, 2062s, 2034s, 2007m, 1952w(br), 1830w(br)	–
2b	2086m, 2062s, 2032s, 2004m, 1950w(br), 1825w(br)	$C_{17}H_8O_{11}Os_3Ru$: C 19.43 (19.26), H 0.89 (0.76)
2c	2088m, 2061s, 2033s, 2004m, 1950w(br), 1830w(br)	$C_{19}H_{12}O_{11}Os_3Ru.CH_2Cl_2$: C 20.35(20.46), H 1.01(1.19)[a]
2d	2084m, 2058s, 2027s, 1998m, 1943w(br), 1821w(br)	$C_{21}H_{16}O_{11}Os_3Ru$: C 22.52 (22.60), H 1.30 (1.44)
2e	2088m, 2061s, 2033s, 2004m, 1951w(br), 1839w(br)	$C_{19}H_{14}O_{11}Os_3RuSi$: C 20.58 (20.41), H 0.83 (1.26)
2f	2084m, 2058s, 2028s, 2000m, 1942w(br), 1828w(br)	$C_{20}H_{14}O_{11}Os_3Ru{\cdot}1.5C_6H_{14}$: C 28.50 (28.27), H 3.21 (2.84)[b]
3	2084m, 2064s, 2032m, 2019m, 2004m, 1948w(br)	$C_{22}H_{12}O_{14}Os_3Ru_2{\cdot}0.5C_6H_{14}$: C 22.98 (22.81), H 1.25 (1.45)[b]
4	2082m, 2055ms, 2026s, 2002m, 1948w(br)	$C_{22}H_{24}O_{10}Os_3RuSi$: C 22.84 (22.99), H 2.33 (2.09)
5	2098vw, 2082w, 2066vs, 2051s, 2043m, 2021m, 2001w	$C_{16}H_{10}O_{11}Os_3Ru$: C 18.05 (18.30), H 0.87 (0.96)
6b	2111w, 2100w, 2080m, 2070ms, 2043s, 2017m, 2000m, 1968w	$C_{17}H_8O_{11}Os_3Ru$: C 19.39 (19.26), H 0.58 (0.76)
6e	2111w, 2100w, 2074m, 2070ms, 2043s, 2016mw, 2000mw, 1968w	$C_{19}H_{14}O_{11}Os_3RuSi$: C 20.44 (20.41), H 1.26 (1.26)

[a] ^{1}H NMR confirmed the presence of dichloromethane in the sample. [b] ^{1}H NMR confirmed the presence of hexane in the sample.

Table 5. ^{1}H NMR spectroscopy and MS data for **2**–**6**.

Cluster	^{1}H NMR, δ [ppm]	MS, *m*/*z* found (calculated) for M^+
2a	5.56 (s, 5 H, Cp), –21.81 (s, 1 H, Os*H*Os)	1045 (1045)
2b	5.62 (m, 2 H, γ-H), 5.46 (m, 2 H, β-H), 1.88 (s, 3 H, Me), –21.60 (s, 1 H, Os*H*Os)	1061 (1060)
2c	4.85 (m, 2 H, γ-H), 4.73 (m, 2 H, β-H), 1.67 (t, $^3J_{HH}$ = 7.5 Hz, 2 H, CH_2), 1.01 (quintet, $^3J_{HH}$ = 7.5 Hz, 2 H, CH_2), 0.58 (t, 3 H, Me, $^3J_{HH}$ = 7.5 Hz), –21.53 (s, 1 H, Os*H*Os)[a]	1088 (1088)
2d	1.25 (s, 15 H, Me), –18.34 (s, 1 H, Os*H*Os)	1116 (1116)
2e	6.15 (m, 2 H, γ-H), 4.99 (m, 2 H, β-H), 0.32 (s, 9 H, Me), –21.21 (s, 1 H, Os*H*Os)	1118 (1118)
2f	5.92 (s, 1 H, Cp), 1.97 (s, 12 H, Me), –20.78 (s, 1 H, Os*H*Os)	1102 (1102)
3	4.78 (m, 1 H), 4.29 (m, 1 H), 4.05 (m, 1 H), 1.18 (m, 2 H), 0.95 (m, 2 H), 0.71 (m, 3 H), –19.54 (br. s, 2 H)[a]	1273 (1273)
4	1.98 (s, 6 H), 1.96(s, 6 H), 0.38 (s, 9 H), –18.46 (s, 3 H)	1147 (1148)
5	4.56 (d, $^3J_{H1H2}$ = 3.2 Hz, 1 H, H^1), 2.93 (dd, $^3J_{H7H6}$ = 15.3 Hz, $^3J_{H7H5}$ = 7.1 Hz, 1 H, H^7), 2.36 (ddd, $^3J_{H2H1}$ = 3.2 Hz, $^3J_{H2H3}$ = 12.2 Hz, $^3J_{H2H4}$ = 6.9 Hz, 1 H, H^2), 2.33 (dd, $^3J_{H3H2}$ = 12.2 Hz, $^3J_{H3H5}$ = 8.2 Hz, 1 H, H^3), 2.17 (ddd, $^3J_{H6H4}$ = 6.9 Hz, $^3J_{H6H5}$ = 11.2 Hz, $^3J_{H6H7}$ = 15.3 Hz, 1 H, H^6), 2.02 (ddd, $^3J_{H4H2}$ = 6.9 Hz, $^3J_{H4H5}$ = 13.0 Hz, $^3J_{H4H6}$ = 8.2 Hz, 1 H, H^4), 1.21 (dddd, $^3J_{H5H3}$ = 8.2 Hz, $^3J_{H5H4}$ = 13.0 Hz, $^3J_{H5H6}$ = 11.2 Hz, $^3J_{H5H7}$ = 7.1 Hz, 1 H, H^5) Major isomer: –13.67 (d, $^2J_{HH}$ = 2.5 Hz, 1 H), –18.97 (d, 1 H), –20.60 (s, 1 H) Minor isomer: –14.47 (s, 1 H), –18.74 (s, 1 H) and –20.73 (s, 1 H)	1049 (1050)
6b	5.21 (s, 1 H), 5.08 (s, 1 H), 4.96 (s, 1 H), 2.13 (s, 3 H), –17.05 (s, br)	1060 (1060)
6e	5.21 (m, 1 H), 5.12 (m, 1 H), 5.04 (m, 1 H), 0.22 (s, 9 H), –17.06 (s, 1 H, Os*H*Os), –17.10 (s, 1 H, Os*H*Os)	1118 (1118)

[a] In C_6D_6.

v/v) gave unreacted **1** (4.1 mg), $Os_3(\mu\text{-}H)_2(CO)_{10}$ (1.3 mg), and a mixture of **2c** and **3** (5.9 mg; **2c**/**3** : 1.3:1.0).

Thermolysis of 2b: To a Carius tube containing cyclohexane (30 mL) was added **2b** (20.2 mg, 0.019 mmol). The reaction mixture was degassed by three freeze-pump-thaw cycles and stirred at 120 °C for 18 h, after which the solvent was removed on the vacuum line. The residue so obtained was redissolved in the minimum of dichloromethane and chromatographed on TLC plates. Elution with hexane/dichloromethane (3:2, v/v) yielded two bands, identified as **6b** (3.6 mg, 18%) and unreacted **2b** (16.2 mg), respectively.

Thermolysis of 2e: To a Carius tube containing cyclohexane (30 mL) was added **2e** (10.7 mg, 0.010 mmol). The reaction mixture was degassed by three freeze-pump-thaw cycles and stirred at 120 °C for 20 h, after which the solvent was removed on the vacuum line. The residue so obtained was redissolved in the minimum of dichloromethane and chromatographed on TLC plates. Elution with hexane/dichloromethane (3:2, v/v) yielded two bands, identified as **6e** (1.5 mg, 14%) and unreacted **2e** (8.7 mg), respectively.

X-ray Crystal Structure Determinations

Crystals were mounted on quartz fibers. X-ray data were collected on a Bruker AXS APEX system, using Mo-K_α radiation, at 223 K with the SMART suite of programs.[29] Data were processed and corrected for Lorentz and polarization effects with SAINT[30] and for absorption effects with SADABS.[31] Structural solution and refinement were carried out with the SHELXTL suite of programs.[32] Crystal and refinement data are summarized in Table 6 and Table 7.

The structures were solved by direct methods to locate the heavy atoms, followed by difference maps for the light, non-hydrogen atoms. There were two molecules in the asymmetric unit for **2a** and **6b**. The hydrides were either located in low-angle difference electron density maps or were placed by potential energy calculations with the program XHYDEX,[22] given fixed isotropic thermal parameters, and were either refined freely, with restraints on the M–H bond lengths, or with a riding model. Organic hydrogen atoms were placed in calculated positions and refined with a riding model. All non-hydrogen atoms were generally given anisotropic displacement parameters in the final model.

Cluster **5** exhibited disorder of the heavy atom positions; the ruthenium atom was modeled as disordered over two sites – M(1) and M(4). The disordered atoms at the same site were given the same coordinate and shifts and thermal parameters, and the Ru occupancy refined and restrained to add up to unity; the refined occupancies were 0.12 and 0.88 for M(1) and M(4), respectively.

 © 2007 Wiley-VCH Verlag GmbH & Co. KGaA, Weinheim

Table 6. Crystal data for **2a**, **2b**, **2d**, **2e**, and **2f**.

Compound	**2a**	**2b**	**2d**	**2e**	**2f**
Formula	$C_{16}H_6O_{11}Os_3Ru$	$C_{17}H_8O_{11}Os_3Ru$	$C_{21}H_{16}O_{11}Os_3Ru$	$C_{19}H_{14}O_{11}Os_3RuSi$	$C_{20}H_{14}O_{11}Os_3Ru$
FW	1045.88	1059.90	1116.01	1118.06	1101.98
Crystal system	orthorhombic	monoclinic	orthorhombic	triclinic	monoclinic
Space group	$P2_12_12_1$	$P2_1/m$	*Pnma*	$P\bar{1}$	$P2_1/m$
Unit cell dimensions					
a [Å]	8.67370(10)	8.4734(3)	19.0091(3)	8.8293(5)	8.940(2)
b [Å]	13.9557(2)	14.4955(5)	14.7068(2)	9.0592(5)	15.324(4)
c [Å]	33.1562(5)	8.6127(3)	8.81410(10)	17.5325(9)	9.186(2)
α [°]	90	90	90	90.960(1)	90
β [°]	90	95.4930(10)	90	91.866(1)	96.021(6)
γ [°]	90	90	90	117.198(1)	90
Volume [Å^3]	4013.48(10)	1053.01(6)	2464.10(6)	1245.85(12)	1251.6(5)
Z	8	2	4	2	2
ρ_c [Mg m^{-3}]	3.462	3.343	3.008	2.980	2.924
μ(Mo-K_α) [mm^{-1}]	19.731	18.803	16.079	15.946	15.826
F(000)	3696	940	2008	1004	988
Crystal size [mm^3]	$0.09\times0.26\times0.36$	$0.20\times0.18\times0.10$	$0.04\times0.32\times0.38$	$0.34\times0.26\times0.02$	$0.19\times0.14\times0.02$
θ range [°]	2.35 to 30.49	2.38 to 30.02	2.55 to 26.37	2.33 to 29.97	2.23 to 26.37
Reflections collected	34822	15665	21261	18903	14131
Independent reflections (R_{int})	11607 [R(int) = 0.0557]	3125 (0.0417)	2612 (0.0968)	7057 (0.0427)	2653 (0.0636)
Completeness%, (to θ [°])	97.2 (30.49)	98.3 (30.02)	100.0 (26.37)	97.1 (29.97)	99.5 (26.37)
Transmission range	0.266–0.115	0.255–0.117	0.528–0.130	0.741–0.074	0.743–0.153
Data/restraints/parameters	11607/0/559	3125/0/169	2612/0/176	7057/0/319	2653/0/170
Goodness-of-fit on F^2	0.984	1.146	1.074	1.060	1.212
Final R indices [$I>2\sigma(I)$]	R_1 = 0.0459	R_1 = 0.0275	R_1 = 0.0394	R_1 = 0.0294	R_1 = 0.0503
	wR_2 = 0.0878	wR_2 = 0.0592	wR_2 = 0.1036	wR_2 = 0.0731	wR_2 = 0.1207
R indices (all data)	R_1 = 0.0520	R_1 = 0.0302	R_1 = 0.0415	R_1 = 0.0336	R_1 = 0.0549
	wR_2 = 0.0897	wR_2 = 0.0601	wR_2 = 0.1052	wR_2 = 0.0751	wR_2 = 0.1234
Absolute structure parameter	0.003(8)	–	–	–	–
Largest diff. peak and hole [e Å^{-3}]	4.114 and –2.175	1.647 and –2.500	2.612 and –4.167	1.421 and –1.450	5.023 and –1.303

Table 7. Crystal data for **3**, **4**, **5**, **6b**, and **6e**.

Compound	**3**	**4**	**5**	**6b**	**6e**
Formula	$C_{22}H_{12}O_{14}Os_3Ru_2$	$C_{22}H_{24}O_{10}Os_3RuSi$	$C_{16}H_{10}O_{11}Os_3Ru$	$C_{17}H_8O_{11}Os_3Ru$	$C_{19}H_{14}O_{11}Os_3RuSi$
FW	1273.06	1148.17	1049.91	1059.90	1118.06
Crystal system	monoclinic	monoclinic	triclinic	monoclinic	triclinic
Space group	$C2/c$	$P2_1/n$	$P\bar{1}$	Cc	$P\bar{1}$
Unit cell dimensions					
a [Å]	14.5019(8)	12.2261(3)	7.7946(3)	8.9642(4)	9.1646(5)
b [Å]	12.9211(7)	14.5775(3)	9.0192(4)	16.7004(7)	12.0684(6)
c [Å]	30.7798(17)	15.9292(3)	15.4979(7)	29.4309(13)	12.3927(6)
α [°]	90	90	94.9330(10)	90	83.407(1)
β [°]	95.998(1)	93.4830(10)	95.9450(10)	93.6030(10)	88.641(1)
γ [°]	90	90	97.3720(10)	90	69.804(1)
Volume [Å^3]	5736.0(5)	2833.75(11)	1069.24(8)	4397.3(3)	1277.69(11)
Z	8	4	2	8	2
ρ_c [Mg m^{-3}]	2.948	2.691	3.261	3.202	2.906
μ(Mo-K_α) [mm^{-1}]	14.337	14.023	18.515	18.011	15.549
F(000)	4576	2088	932	3760	1004
Crystal size [mm^3]	$0.34\times0.20\times0.16$	$0.38\times0.34\times0.18$	$0.10\times0.17\times0.36$	$0.28\times0.18\times0.16$	$0.38\times0.24\times0.05$
θ range [°]	2.12 to 26.37	2.04 to 30.02	2.29 to 30.51	2.44 to 29.55	2.31 to 30.00
Reflections collected	43335	23997	15556	16172	19422
Independent reflections (R_{int})	5861 (0.0423)	8098 (0.0346)	6282 (0.0462)	8336 (0.0257)	7215 (0.0353)
Completeness%, (to θ [°])	100.0 (26.37)	97.6 (30.02)	96.2 (30.51)	91.4 (29.55)	96.8 (30.00)
Transmission range	0.208–0.085	0.187–0.076	0.266–0.122	0.161–0.081	0.510–0.067
Data/restraints/parameters	5861/0/370	8098/0/344	6282/6/309	8336/2/579	7215/0/331
Goodness-of-fit on F^2	1.434	1.053	1.015	1.061	1.051
Final R indices [$I>2\sigma(I)$]	R_1 = 0.0702	R_1 = 0.0311	R_1 = 0.0332	R_1 = 0.0274	R_1 = 0.0290
	wR_2 = 0.1561	wR_2 = 0.0717	wR_2 = 0.0683	wR_2 = 0.0706	wR_2 = 0.0701
R indices (all data)	R_1 = 0.0727	R_1 = 0.0398	R_1 = 0.0405	R_1 = 0.0286	R_1 = 0.0338
	wR_2 = 0.1569	wR_2 = 0.0747	wR_2 = 0.0705	wR_2 = 0.0712	wR_2 = 0.0751
Largest diff. peak and hole [e Å^{-3}]	2.251 and –2.606	2.237 and –2.123	2.196 and –1.747	1.430 and –1.422	1.555 and –1.668

 © 2007 Wiley-VCH Verlag GmbH & Co. KGaA, Weinheim

CCDC-634245 to CCDC-634254 contain the supplementary crystallographic data for this paper. These data can be obtained free of charge from The Cambridge Crystallographic Data Centre via www.ccdc.cam.ac.uk/data_request/cif.

Acknowledgments

This work was supported by the National University of Singapore (Research Grant No. R143–000–190–112) and one of us (Y. L. K. T.) thanks the University for a Research Scholarship.

[1] B. F. G. Johnson, J. Lewis, C. E. Housecroft, M. A. Gallop, M. Martinelli, D. Braga, F. Grepioni, *J. Mol. Catal.* **1992**, *74*, 61–72.
[2] a) E. L. Muetterties, T. L. Rhoden, E. Band, C. F. Bruker, W. R. Pretrzer, *Chem. Rev.* **1979**, *79*, 91–137; b) H. Wadepohl, *Angew. Chem. Int. Ed. Engl.* **1992**, *31*, 247–262; c) B. F. G. Johnson, M. A. Gallup, Y. V. Roberts, *J. Mol. Catal.* **1994**, *86*, 51–69; d) B. F. G. Johnson, *J. Organomet. Chem.* **1994**, *475*, 31–43; e) P. J. Dyson, J. S. McIndoe, *Transition Metal Carbonyl Cluster Chemistry*, Gordon and Breach, The Netherlands, **2000**.
[3] a) L. Pereira, W. K. Leong, S. Y. Wong, *J. Organomet. Chem.* **2000**, *609*, 104–109; b) L. J. Pereira, K. S. Chan, W. K. Leong, *J. Organomet. Chem.* **2005**, *690*, 1033–1043; c) L. J. Pereira, W. K. Leong, *J. Organomet. Chem.* **2006**, *691*, 1941–1944; d) L. J. Pereira, W. K. Leong, *J. Organomet. Chem.* **2006**, *691*, 2448–2456; e) L. J. Pereira, W. K. Leong, *Polyhedron* **2006**, *25*, 2392–2400.
[4] a) Y. L. K. Tan, W. K. Leong, *J. Organomet. Chem.* **2006**, *691*, 2048–2054; b) Y. L. K. Tan, C. W. A. Koh, T. B. Lim, W. K. Leong, *J. Cluster Sci.* **2006**, *17*, 509–516; c) Y. L. K. Tan, W. K. Leong, *J. Organomet. Chem.* **2007**, *692*, 768–772.
[5] a) H. Wadepohl, S. Gebert, H. Pritzkow, *J. Organomet. Chem.* **2000**, *614–5*, 158–167; b) P. J. Dyson, B. F. G. Johnson, C. M. Martin, *Coord. Chem. Rev.* **1996**, *155*, 69–86; c) M. Castiglioni, R. Giordano, E. Sappa, *J. Organomet. Chem.* **1995**, *491*, 111–120; d) B. F. G. Johnson, *J. Organomet. Chem.* **1994**, *475*, 31–43.
[6] R. Buntem, J. Lewis, C. A. Morewood, P. R. Raithby, M. C. R. de Arellano, G. P. Shields, *J. Chem. Soc., Dalton Trans.* **1998**, 1091–1096.
[7] a) M. R. Churchill, B. G. DeBoer, F. J. Rotella, *Inorg. Chem.* **1976**, *15*, 1843–1853; b) R. Bau, R. G. Teller, S. W. Kirtley, T. F. Koetzle, *Acc. Chem. Res.* **1979**, *12*, 176–186; c) D. J. Elliot, J. J. Vittal, R. J. Puddephatt, D. G. Holah, A. N. Hughes, *Inorg. Chem.* **1992**, *31*, 1247–1250; d) R. D. Adams, J. P. Selegue in *Comprehensive Organometallic Chemistry* (Eds.: G. Wilkinson, F. G. A. Stone, E. W. Abel), Pergamon, **1982**, vol. 4.
[8] a) J. Lewis, C. A. Morewood, P. R. Raithby, M. C. R. de Arellano, *J. Chem. Soc., Dalton Trans.* **1996**, 4509–4510; b) J. Lewis, C. A. Morewood, P. R. Raithby, M. C. R. de Arellano, *J. Chem. Soc., Dalton Trans.* **1997**, 3335–3342.
[9] W. Wang, H. B. Davis, F. W. B. Einstein, R. K. Pomeroy, *Organometallics* **1994**, *13*, 5113–5121.
[10] J. A. Iggo, *NMR Spectroscopy in Inorganic Chemistry*, Oxford University Press, Oxford, **1999**.
[11] H. G. Ang, L. L. Koh, G. Y. Yang, *J. Chem. Soc., Dalton Trans.* **1996**, 1573–1581.
[12] M. R. A. Al-Mandhary, J. Lewis, P. R. Raithby, *J. Organomet. Chem.* **1997**, *530*, 247–250.
[13] J. P. Canal, G. P. A. Yap, R. K. Pomeroy, *Organometallics* **2003**, *22*, 3439–3447.
[14] R. Buntem, J. F. Gallagher, J. Lewis, P. R. Raithby, M. A. Rennie, G. P. Shields, *J. Chem. Soc., Dalton Trans.* **2000**, 4297–4303.
[15] R. K. Pomeroy in *Comprehensive Organometallic Chemistry II* (Eds.: G. Wilkinson, F. G. A. Stone, E. W. Abel), Pergamon Press, **1995**, vol. 7, ch. 15.
[16] a) J. R. Fox, W. L. Gladfelter, T. G. Wood, J. A. Smegal, T. K. Foreman, G. L. Geoffroy, I. Tavanaipour, V. W. Day, C. S. Day, *Inorg. Chem.* **1981**, *20*, 3214–3224; b) W. L. Gladfelter, G. L. Geoffroy, *Inorg. Chem.* **1980**, *19*, 2579–2585.
[17] Y. Chi, C.-Y. Cheng, S.-L. Wong, *J. Organomet. Chem.* **1989**, *378*, 45–56.
[18] a) H. Chen, B. F. G. Johnson, J. Lewis, D. Braga, F. Grepioni, E. Parasini, *J. Chem. Soc., Dalton Trans.* **1991**, 215–219; b) S. Bhaduri, B. F. G. Johnson, J. W. Kelland, J. Lewis, P. R. Raithby, S. Rehani, G. M. Sheldrick, K. Wong, M. McPartlin, *J. Chem. Soc., Dalton Trans.* **1979**, 562–568; c) B. F. G. Johnson, A. J. Blake, C. M. Martin, D. Braga, E. Parasini, H. Chen, *J. Chem. Soc., Dalton Trans.* **1994**, 2167–2175.
[19] B. F. G. Johnson, J. Lewis, A. G. Orpen, P. R. Raithby, K. D. Rouse, *J. Chem. Soc., Dalton Trans.* **1981**, 788–792.
[20] a) J. J. Guy, B. E. Reichert, G. M. Sheldrick, *Acta Crystallogr., Sect. B* **1976**, *32*, 3319–3320; b) A. G. Orpen, D. Pippard, G. M. Sheldrick, K. D. Rouse, *Acta Crystallogr., Sect. B* **1978**, *34*, 2466–2472; c) R. J. Goudsmit, B. F. G. Johnson, J. Lewis, P. R. Raithby, *Acta Crystallogr., Sect. B* **1982**, *38*, 2689–2691.
[21] M. B. Smith, J. March, *March's Advanced Organic Chemistry*, 5th ed., Wiley, New York, **2001**.
[22] A. G. Orpen, *XHYDEX*, School of Chemistry, University of Bristol, UK, **1997**.
[23] a) M. R. Churchill, B. G. DeBoer, *Inorg. Chem.* **1977**, *16*, 878–884; b) B. F. G. Johnson, J. Lewis, P. R. Raithby, G. M. Sheldrick, K. Wong, M. McPartlin, *J. Chem. Soc., Dalton Trans.* **1978**, 673–676.
[24] D. B. Brown, B. F. G. Johnson, C. M. Martin, A. E. H. Wheatley, *J. Chem. Soc., Dalton Trans.* **2000**, 2055–2060.
[25] a) R. Della Pergola, L. Garlaschelli, M. Manassero, M. Sansoni, A. Sironi, D. Strumolo, *J. Organomet. Chem.* **2005**, *690*, 4768–4772; b) Y.-C. Liu, W.-Y. Yeh, G.-H. Lee, S.-M. Peng, *J. Organomet. Chem.* **2004**, *689*, 1944–1948; c) J. B. Keister, J. R. Shapley, *J. Am. Chem. Soc.* **1976**, *98*, 1056–1057; d) A. J. Deeming, M. Underhill, *J. Chem. Soc., Dalton Trans.* **1974**, 1415–1419; e) B. F. G. Johnson, J. W. Kelland, J. Lewis, S. K. Rehani, *J. Organomet. Chem.* **1976**, *113*, C42–44.
[26] M. A. Gallop, B. F. G. Johnson, J. Lewis, P. R. Raithby, *J. Chem. Soc., Chem. Commun.* **1986**, *9*, 706–708.
[27] L. R. Martin, F. W. B. Einstein, R. K. Pomeroy, *Inorg. Chem.* **1988**, *27*, 2986–2989.
[28] W. Wang, F. W. B. Einstein, R. K. Pomeroy, *Organometallics* **1993**, *12*, 3079–3086.
[29] *SMART* version 5.628, Bruker AXS Inc., Madison, Wisconsin, USA, **2001**.
[30] *SAINT+* version 6.22a, Bruker AXS Inc., Madison, Wisconsin, USA, **2001**.
[31] G. M. Sheldrick, *SADABS*, **1996**.
[32] *SHELXTL* version 5.1, Bruker AXS Inc., Madison, Wisconsin, USA, **1997**.

Received: January 22, 2007
Published Online: April 10, 2007

 © 2007 Wiley-VCH Verlag GmbH & Co. KGaA, Weinheim